Albert et al., http://www.jcb.org/cgi/content/full/jcb.201208186/DC1

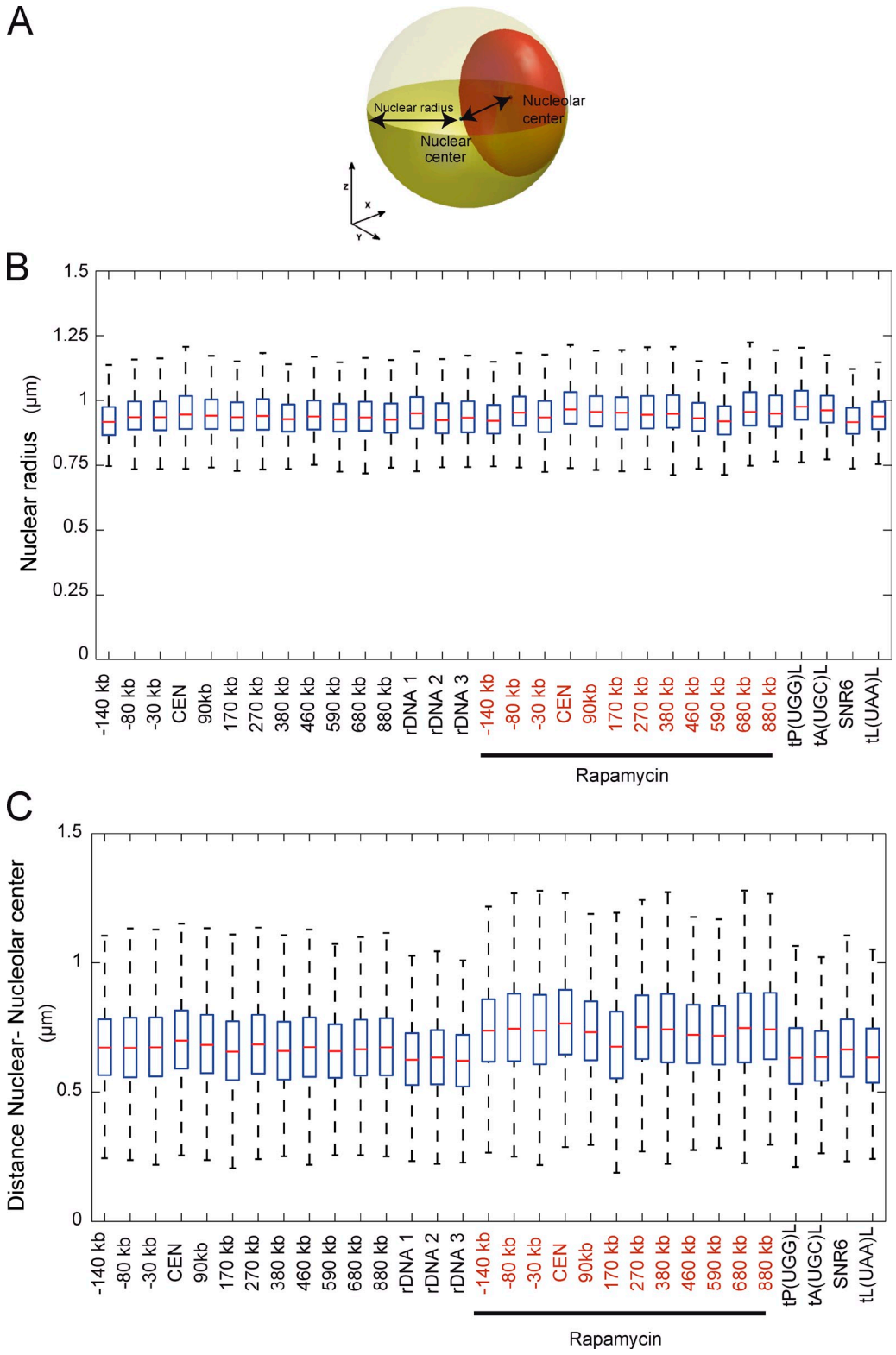

Figure S1. **Nuclear morphology of the 31 populations analyzed encompassing 15 FROS-tagged strains in exponentially growing cells, 10 rapamycin-treated FROS strains for 20 min, and four exponentially growing strains bearing FROS-labeled Pol III–transcribed genes along yeast chromosome XII.** (A) Schematic representation of nuclear radius and distances separating nuclear and nucleolar centers in the cell population measured in 3D using the gene map method (Berger et al., 2008). (B and C) Box plot of nuclear radius (B) and distance between nuclear–nucleolar centers (C) in each of the 31 populations analyzed are shown. Nuclear morphology is comparable in each cell population, except for an increase in nuclear–nucleolar center distances when rapamycin treatment is applied

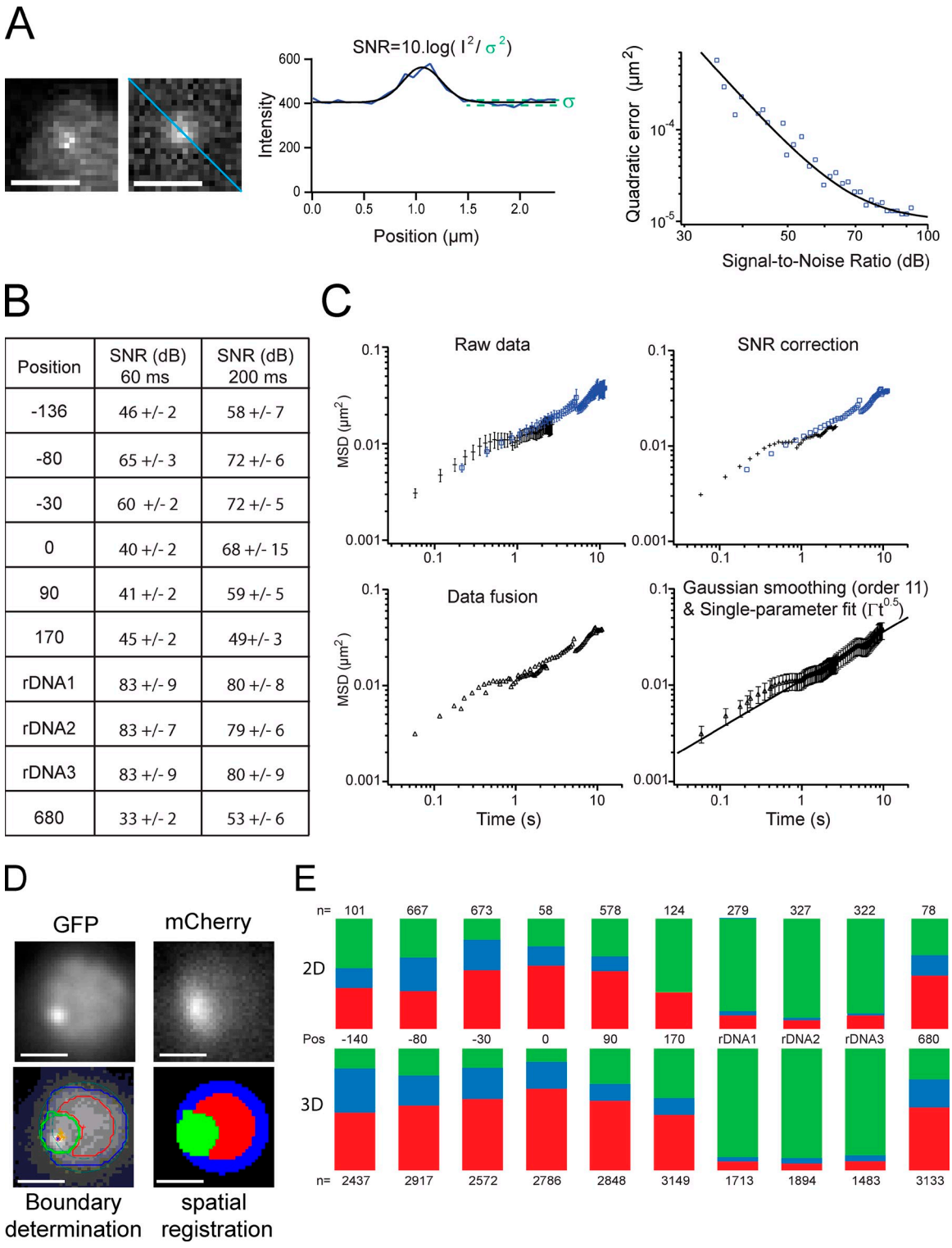

Position	SNR (dB) 60 ms	SNR (dB) 200 ms
-136	46 +/- 2	58 +/- 7
-80	65 +/- 3	72 +/- 6
-30	60 +/- 2	72 +/- 5
0	40 +/- 2	68 +/- 15
90	41 +/- 2	59 +/- 5
170	45 +/- 2	49+/- 3
rDNA1	83 +/- 9	80 +/- 8
rDNA2	83 +/- 7	79 +/- 6
rDNA3	83 +/- 9	80 +/- 9
680	33 +/- 2	53 +/- 6

Figure S2. **Tracking loci in living cells.** (A) Our approach to evaluating the SNR and its impact on single particle tracking. Fluorescent loci appear as point-like structures, as shown in the left image. Such images can be generated in silico (second image), after the definition of the background and the maximal intensity of the tracer (bars, 1 µm). The intensity along the blue line in the image is represented in the middle panel, and the definition of the SNR is appended in the inset. We then compare the quadratic localization error by measuring the difference in position between the simulated object and the measurement derived from the software (plot on the right), and show that the localization error is reduced as the SNR increases (the line is a guide to the eye). Robustness of measurements is illustrated by individual in silico detection (blue boxes). (B) In the table, the measured SNR from time-lapse acquisitions is reported for each locus, and for fast (60 ms) or slow (200 ms) acquisitions. (C) For locus −136 (central localization, shown in Fig. S3), we show the process flow to generate MSD, starting from raw data with the error bars (top left). We then compensate for the difference in SNR according to our calibration presented in A (note that the variations in localization errors between the acquisitions at different acquisition rates are minimal) and fuse the datasets (bottom left). We finally filter the fused data with the error bars using Gaussian smoothing (order 11; bottom), and fit the data with a model of anomalous diffusion (black line). (D) Spatial registration of cell nucleus based on two-color imaging of GFP-Tet and mCherry-Nop1 signals. For each cell, the nucleus is automatically segmented with the Canny filter to define central, peripheral, and nucleolar regions, respectively, as red, blue, and green regions. Note that the three nuclear regions were defined as: the region delimited by a circle of 1.1 × the NUC radius for the NUC, the region located at distances <0.31 × the nuclear radius from the periphery for the peripheral location, and the remaining region for the center (right). (E) The proportion of trajectories found in nucleolar, central, or peripheral regions using the tracking software (top) is compared with the proportion of loci determined in 3D with the gene map method (Berger et al., 2008). In the case of gene maps, note that loci are considered to be nucleolar when positioned within 100 nm from segmented NUC, peripheral if <100 nm from the NE, and otherwise central.

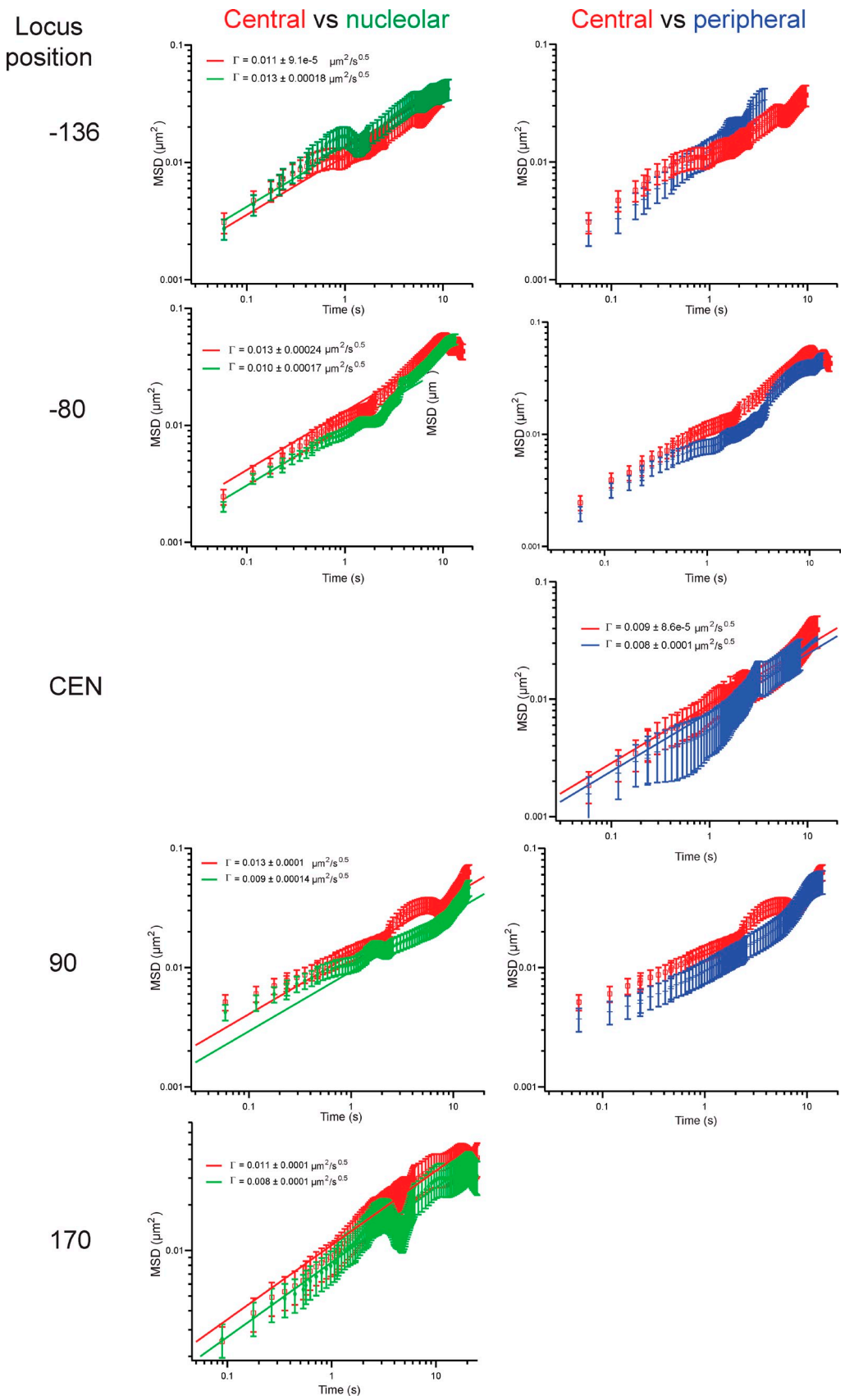

Figure S3. **MSD responses for loci −136 kb, −80 kb, CEN, 90 kb, and 170 kb along chromosome XII.** On the left, we plotted the MSD response for a central or nucleolar localization (red and green datasets, respectively). The same plot for a central and a peripheral localization is shown on the right (red and blue dataset, respectively). These data were adjusted with an anomalous diffusion model with one adjustable parameter in $\Gamma t^{0.5}$. Note that the MSD datasets for genes located at −30 kb, 680 kb, and in the rDNA are represented in Fig. 4. Nucleolar and peripheral trajectories were not obtained for loci CEN and 170, respectively.

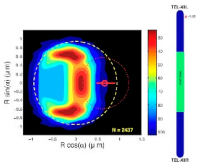

Video 1. **Overlay of color-coded statistical mapping of loci positions along chromosome XII.** The spatial distributions of each locus are represented as a color-coded heat map determined by the percentile of the distribution (Berger et al., 2008; Therizols et al., 2010). The dashed yellow circle, the dashed red circle, and the small, solid red circle depict the median NE, the median NUC, and the median location of the nucleolar center, respectively. Chromosome XII with the 12 FROS-labeled loci is schematically represented using the centromere as the origin (right). Time delay between each statistical mapping is proportional to distances in kilobases separating each locus. The overlay was generated using After Effects CS6 (Adobe).

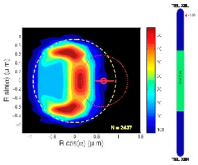

Video 2. **Interpolation between color-coded statistical maps of loci positions along chromosome XII.** Interpolation along the entire chromosome was achieved for each percentile color level independently, using After Effects CS6 software (Adobe). One statistical map with 1-kb resolution was then obtained for the entire chromosome, excluding rDNA. The dashed yellow circle, the dashed red circle, and the small, solid red circle depict the median NE, the median NUC, and the median location of the nucleolar center, respectively.

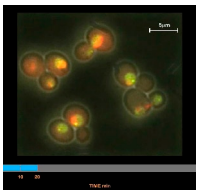

Video 3. **Long-term motion of one locus of chromosome XII in budding yeast.** The *S. cerevisiae* strain (HBT24-1a) bears one labeled locus (position 90 kb), a GFP-tagged nuclear pore complex labeling nuclear envelop (Nup49-GFP), and a red nucleolar marker (mCherry-Nop1). Images were acquired by time-lapse microscopy, using a wide-field microscope (Ti-E/B; Nikon). Frames for GFP were taken every 10 s. Bright-field and mCherry signals were acquired every 100 s. For visualization purposes, red and bright-field images were refreshed every 10 GFP frames. The movie was set to 24 images per second, resulting in an apparent 240-fold speed increase. Note that nuclear size increases with cell cycle progression, and that nuclei move rapidly during mitosis. Images were processed for visualization (see Material and methods).

Table S1. **Yeast strains**

FROS position/ genome position	FROS position/ CEN as origin	Name	Genotype	Origin
WT	WT	ODN1-1a	*MATa his3Δ1 leu2Δ0 met15Δ0 ura3Δ0 trp1Δ0*	This study
		Nucloc2	*MATα his3Δ0 leu2Δ1 ura3-Δ851 ade2-801 lys2-Δ202::GFP::TETR-LYS2 nup49Δ::HPHMX3* + pASZ11-NupNop	Berger et al., 2008
Untagged	Untagged	TMS1_1a	*MATa* his3-Δ1, leu2-Δ1, ura3-Δ0, ade2-801, lys2-801,LYS2::TETR-GFP, nup49-Δ::HPH-MX6 + pASZ11-NupNop	Offspring of ODN1-1a × NucLoc2
Chr XII −014 kb	Chr XII −136 kb	Ben1_2a	*MATa his3-Δ1, leu2-Δ1, ura3-Δ0, ade2-801, lys2-801,LYS2::TETR-GFP, nup49-Δ::HPH-MX6, interPAU18-AYT1::his3::TetO-NAT* + pASZ11-NupNop	This study
Chr XII 070 kb	Chr XII −80 kb	Jez15_1a	*MATa his3-Δ1, leu2-Δ1, ura3-Δ0, ade2-801, lys2-801,LYS2::TETR-GFP, nup49-Δ::HPH-MX6, interGRC3-RIX7::ura3::TetO-NAT* + pASZ11-NupNop	This study
Chr XII 120 kb	Chr XII –30 kb	ICH5_1a	*MATa* his3-Δ1, leu2-Δ1, ura3-Δ0, ade2-801, lys2-801,LYS2::TETR-GFP, nup49-Δ::HPH-MX6, *interYLL014w-YLL013c::TetO-NAT* + pASZ11-NupNop	This study
Chr XII 150 kb	Chr XII 0 kb	Jez11_1a	*MATa his3-Δ1, leu2-Δ1, ura3-Δ0, ade2-801, lys2-801,LYS2::TETR-GFP, nup49-Δ::HPH-MX6, interDNM1-cen::his3::TetO-NAT* + pASZ11-NupNop	This study
Chr XII 240 kb	Chr XII 90 kb	HBT24_1a	*MATa* his3-Δ1, leu2-Δ1, ura3-Δ0, ade2-801, lys2-801,LYS2::TETR-GFP, nup49-Δ::HPH-MX6, *interYLR048W-YLR049C::his3::TetO-Nat* + pASZ11-NupNop	This study
Chr XII 320 kb	Chr XII 170 kb	Ben3_1a	*MATa his3-Δ1, leu2-Δ1, ura3-Δ0, ade2-801, lys2-801,LYS2::TETR-GFP, nup49-Δ::HPH-MX6, interYLR092w-YLR093c::his3::TetO-NAT* + pASZ11-NupNop	This study
Chr XII 420 kb	Chr XII 270 kb	HBT27_1a	*MATa* his3-Δ1, leu2-Δ1, ura3-Δ0, ade2-801, lys2-801,LYS2::TETR-GFP, nup49-Δ::HPH-MX6, *interYLR143w-YLR144c::ura3::TetO-Nat* + pASZ11-NupNop	This study
Chr XII 530 kb	Chr XII 380 kb	Jez14_1a	*MATa his3-Δ1, leu2-Δ1, ura3-Δ0, ade2-801, lys2-801,LYS2::TETR-GFP, nup49-Δ::HPH-MX6, interYLR188w-YLR189c::ura3::TetO-NAT+* pASZ11-NupNop	This study
Chr XII 610 kb	Chr XII 460kb	HBT28_1a	*MATa* his3-Δ1, leu2-Δ1, ura3-Δ0, ade2-801, lys2-801,LYS2::TETR-GFP, nup49-Δ::HPH-MX6, i*nterYLR238W-YLR239C::his3::TetO-Nat* + pASZ11-NupNop	This study
Chr XII 740 kb	Chr XII 590 kb	Ben5_1a	*MATa his3-Δ1, leu2-Δ1, ura3-Δ0, ade2-801, lys2-801,LYS2::TETR-GFP, nup49-Δ::HPH-MX6, interYLR307w-YLR307c-a::his3::TetO-NAT* + pASZ11-NupNop	This study
Chr XII 830 kb	Chr XII 680 kb	Jez1_1a	*MATa his3-Δ1, leu2-Δ1, ura3-Δ0, ade2-801, lys2-801,LYS2::TETR-GFP, nup49-Δ::HPH-MX6, interYLR353w-YLR354c::his3::TetO-NAT* + pASZ11-NupNop	This study
Chr XII 1,030 kb	Chr XII 880 kb	HBT30_1a	*MATa* his3-Δ1, leu2-Δ1, ura3-Δ0, ade2-801, lys2-801,LYS2::TETR-GFP, nup49-Δ::HPH-MX6, *interYLR451w-YLR452c::his3::TetO-NAT* + pASZ11-NupNop	This study
ChrXII-rDNA1	Chr XII-rDNA	Ben51_1a	*MATa his3-Δ1, leu2-Δ0, C, ura3-Δ0, ade2-801, lys2801,LYS2::TETR-GFP, nup49-Δ::HPH-MX6 inter rDNA ura3::TetO-NAT+ pASZ11-NupNop*	This study
ChrXII-rDNA2	Chr XII-rDNA	Ben52_1a	*MATa his3-Δ1, leu2-Δ0, C, ura3-Δ0, ade2-801, lys2801,LYS2::TETR-GFP, nup49-Δ::HPH-MX6 inter rDNA ura3::TetO-NAT+ pASZ11-NupNop*	This study
ChrXII-rDNA3	Chr XII-rDNA	Ben57_1a	*MATa his3-Δ1, leu2-Δ0, C, ura3-Δ0, ade2-801, lys2801,LYS2::TETR-GFP, nup49-Δ::HPH-MX6 inter rDNA ura3::TetO-NAT+ pASZ11-NupNop*	This study
SNR6	Chr XII 210 kb	yCNOD15-1c	*MATa* his3-Δ1, leu2-Δ0, ura3-Δ0, ade2-801, lys2-801,LYS2::TETR-GFP, nup49-Δ::HPH-MX6 interSNR6-YLR108c::his3::TetO-NATMX6 + pASZ11-NupNop	This study
tP(UGG)L	Chr XII −60 kb	yCNOD123-1a	MATa his3-Δ1, leu2-Δ1, ura3-Δ0, ade2-801, lys2-801,LYS2::TETR-GFP, nup49-Δ::HPH-MX6, inter tP(UGG)L-PAU17::his3::TetO-Nat + pASZ11-NupNop	This study
tA(UGC)L	Chr XII 60 kb	yCNOD124-1a	MATa his3-Δ1, leu2-Δ1, ura3-Δ0, ade2-801, lys2-801,LYS2::TETR-GFP, nup49-Δ::HPH-MX6, inter tA(UGC)L-MLH2::ura3::TetO-Nat + pASZ11-NupNop	This study
tL(UAA)L	Chr XII 810 kb	yCNOD125-1a	MATa his3-Δ1, leu2-Δ1, ura3-Δ0, ade2-801, lys2-801,LYS2::TETR-GFP, nup49-Δ::HPH-MX6, inter tL(UAA)L-YLR419w::ura3::TetO-Nat + pASZ11-NupNop	This study

Chr, chromosome; WT, wild type.

Table S2. **Oligonucleotides used in this study**

Number	Name	Genomic position	Sequence (5′–3′)
558	chrXII-014K-M13F	interPAU18-AYT1	AATTTCATCGTCTTATATTTCGATAATAAAACAATACAGTGAGCGTTGTTATTAAGTAAATCATAGGCACTTGGTATCATGTAAAACGACGGCCAGT
559	chrXII-014K- M13R	interPAU18-AYT1	TCAATAAGGAGATGAACTAGGCCATCAACAATTACTAACACGCACACACGCACTACTACAACTACTTGATTTTGAATTATGGAAACAGCTATGACCATG
610	o-chrXII-70k-M13F	interGRC3-RIX7	CGTCATGAGACGTGGCCAATTCATGAAAAGATAGAAAGAAAAGGTAATCGTACATTTTTTAATAGTGAAAGATAGAGGATACAGTAAAACGACGGCCAGT
611	o-chrXII-70k-M13R	interGRC3-RIX7	GTCCCTAGAAGTTAGTATGACTTAGATATTGAAGGAATATGAGTATACATAACAAATATATAAAACTTTGCATGATTTTTGGGAAACAGCTATGACCATG
560	o-chrXII120k	interYLL014W-YLL013C	ACATGACAACAGTATTCTCAGTCAAATGATTTCAAATACACAATGTTAAATTCTCTATCTGTTGCAGAAATAAGAAGAGCGTAAAACGACGGCCAGT
561	o-chrXII120k-rev	interYLL014W-YLL013C	ATATTCATTATTTGCTTTTTTCCATTACCTACTTTTTGTACCTCATCTCTATTTTTCTGCAAAAATCTTTGCGCTCTTACGGAAACAGCTATGACCATG
606	o-chrXII150k-M13F	interDNM1-cen	TTATAGGTCAGTGTTTATTCCTTTACTCAGTTGATGATTTCAAATGTGCTCTCCTCTCCATTCTTTTTCTTGTTAATAAAAATGTAAAACGACGGCCAGT
607	o-chrXII150k-M13R	interDNM1-cen	GGTAGAGCTTCTCTAGTGAAGGTTCTCTAGCTTAGTTAATACTTTTGCGATTGCTAATATTTGTTATTTATTTAGTTATGGGGAAACAGCTATGACCATG
562	o-chrXII24k	interYLR048W-YLR049C	TTTTTTATTAGGTAAGTGGTTTCAATAATTAAATTCTTTAGCGGGAAGGCTGACTATCTATAGTATTGAAGATAAGTTAAGTAAAACGACGGCCAGT
563	o-chrXII24krev	interYLR048W-YLR049C	AATACTCGGGTGAACCCGTCATGGCGAATAGTGCAAATTTAATTAATAATAAAAATGAAATATCAGAACTAAACATTAATGGAAACAGCTATGACCATG
564	o-chrXII32k	interYLR092W-YLR093C	TCATAATGAGATAGACACTGTTTATATAATAAGAAATAATAGGTAGGATGGTGCCATCGTGAGCATATACATACCTATAAGTAAAACGACGGCCAGT
565	o-chrXII32krev	interYLR092W-YLR093C	ACGACAATAACATTAATAACGGTTGTATTTCTTTTGTTCCTGAGAGGAAGAGAAAAATAAAATAAAAATAAGGTAAATATGGAAACAGCTATGACCATG
566	o-chrXII42k	interYLR143W-YLR144C	ATACGCTGTCCACGCTCCTGGCGGTGTAAATGATAGACAGATCCCAAATATGTTAGCAAATCATAGGAACAACACCATATGTAAAACGACGGCCAGT
567	o-chrXII42krev	interYLR143W-YLR144C	TCCTAAACCATCATCAATAATCAAATTATTACAGAACACACCTTAATTGTGCGGCGTATTCTAAATTTTACGTGTTCACAGGAAACAGCTATGACCATG
568	o-chrXII53k	interYLR188W-YLR189C	TCCTTGTACGCCTTTATACACATTAAATTAATATTAGATGCACAACATACGGTACGTTTAGGAAACTCAAATTAAGCTTTAGTAAAACGACGGCCAGT
569	o-chrXII53krev	interYLR188W-YLR189C	AAGTTTCAGTCATATTTGTACTCAGGAAAGATATGAAAACGATAATGTTGATAATAAGAATAATAGTAACAATAATGGAAACAGCTATGACCATG
570	o-chrXII61k	interYLR238W-YLR239C	TTTCCCCCAACTAGCATCGTAAATACAAGACACACACGATCCGCTTTTCACGTCAGAGATTATTATATACGTACGTATATGTAAAACGACGGCCAGT
571	o-chrXII61krev	interYLR238W-YLR239C	TCCGTGAGACGGATGACTCCCCCCATACTTTCTTAAATGAAAGGATGCTTACCTTTTTTTACATGTGAATATCTATTACATGGAAACAGCTATGACCATG
572	o-chrXII74k	interYLR307W-YLR307C-A	AGTATGTATTAGAATAGAGGACATATATAAAAATCATATATATCGATGCTTGAATGTATAAGGAAAAGCGTCAAATTATGGTAAAACGACGGCCAGT
573	o-chrXII74krev	interYLR307W-YLR307C-A	CTAAAAGATTCTAAAAAATTACTTTTTAAAGTTATACCCTCTGACTTTATGTGACATCAGCATCCTAAGTACCTACCGTTGGAAACAGCTATGACCATG
574	o-chrXII83k	interYLR353W-YLR354C	AAACTGTTCTGTCTCGTTAAAGTCATATATATAAATAGGGGATTTTCATTAATTTATATATATAGATATACTTGTGTACAGTAAAACGACGGCCAGT
575	o-chrXII83krev	interYLR353W-YLR354C	TTACCGCTTAAGGAAGTATCTCGGAAATATTAATTTAGGCCATGTCCTTATGCACGTTTCTTTTGATACTTACGGGTACAGGAAACAGCTATGACCATG
576	o-chrXII1030k	interYLR451W-YLR452C	CAGACGGACTTAAACCGCCAACCAGCCTTGGCCACAGGTGTATGATGCGAAGATTCGTAAGCGCTCACGTTAGTCACATCGTAAAACGACGGCCAGT
577	o-chrXII1030krev	interYLR451W-YLR452C	AGCGGAGGTGTGATTTGTTATATCAACTATAATATGATTAAATAAAGCCATTTATTATCTAGTATAATTTCCAATCCTGAGGAAACAGCTATGACCATG
1033	URA3_M13F-SceI	Construction of SI-SceI-URA3.	AAAAAAGGATCCGGTATCGATAAGCTTGATGTATTACCCTGTTATCCCTAGCGTATGTGGCTGTGGTTTCAGGGTCCAT
1034	URA3_M13R	Construction of SI-SceI-URA3.	TTTTTGTCGACCCCGGGCTGCAGGAATTCGATTGT
1035	rDNA-M13F.	Tagging of rDNA.	AGCAGTTTTTTCCGCACCATCAGAGCGGCAAACATGAGTGCTTGTATAAGTTTAGAGAATTGAGAAAAGCTCATTTCCTATAGGTAAAACGACGGCCAGT
1036	rDNA-M13R	Tagging of rDNA.	TCACTGTTCACTTGTCTCTTACATCTTTCTTGGTAAAATCGTAGTTCGTAGTATTTTTTTTCATATCAAAGGCATGTCCTGGGAAACAGCTATGACCATG
528	o-M13F_SNR6	interSNR6-YLR108c	TGAATGTGAATATTGTTACAGCTATGCAATGGTACGATCATACTCTGAACGATCCATTTAAATTATATATGTAAAACGACGGCAGT
529	o-M13R_SNR6	interSNR6-YLR108c	GAAGGAATATTGCAAAATGATTGATTTTCTGTGAAATCTTCAATAAAAAAACCTTTCTCTTCTGTTTGACGGAAACAGCTATGACCATG
1240	tP(UGG)L-rev	inter tP(UGG)L-PAU17	GCACAAACTGAGGATTCTCAGCCTTCCTACGGCATAATCCTTTATAATTATTGTTTTAGCCCAGGAAACAGCTATGAC

Table S2. **Oligonucleotides used in this study** *(Continued)*

Number	Name	Genomic position	Sequence (5′–3′)
1241	tP(UGG)L_fw	inter tP(UGG)L-PAU17	TTACAACTAATGGTATGCAATTCATAAAGCATAGGCCAAAAGACCCTGATACAGA TATATGTAAAACGACGGCCAGT
1244	tA(UGC)L-fw	inter tA(UGC)L-MLH2	ACAGTAAAAGCAAAAAAGCATTGTGCCAGGGCAATATAGCGAGCACTACTTAA ACCCAAAGTAAAACGACGGCCAGT
1245	tA(UGC)L-rev	inter tA(UGC)L-MLH2	GATTACCTTCTGCATTATCTATAAGTTTTGCGCATAACAAACCTTTCACTTGTCACCT AACCAGGAAACAGCTATGAC
1250	tL(UAA)L-rev	inter tL(UAA)L-YLR419w	AAAGACAATGTGCTATGTAGTTTACGGGATTCTAGCCCTGATTCAGCAAAGAGA AAAACACCAGGAAACAGCTATGAC
1251	tL(UAA)L-fw	inter tL(UAA)L-YLR419w	CATATAGAAGTGTCAAAGTATAAAACACTAACAAAAATCTAAGAGATTATTGCGAC TGCGGTAAAACGACGGCCAGT
	SNR6_HindIII_F	Probe for IEL	AGCTTTAAAGGCTCTGATTTTGGATTCG
	SNR6_HindIII_R	Probe for IEL	CACAGCATGGATACTGATGGTTCTTGGT
	SNR6	Oligo For RT (98 bp product)	TCTCTTTGTAAAACGGTTCATCCT
	SNR14 (U4 control)	Oligo For RT (115 bp product)	GCGAACACCGAATTGACCATG

Table S3. **Plasmids used in this study**

Name	Reference
pTetO-Nat-HIS3Δ	Berger et al., 2008
pTetO-Nat-URA3Δ	Berger et al., 2008
pCR4-HIS3-M13	Berger et al., 2008
pSK-URA3-M13	Berger et al., 2008
pASZ11-GFP-NUP49-NOP1-Cherry	Berger et al., 2008
pSK-URA3-SceI-M13	This study

References

Berger, A.B., G.G. Cabal, E. Fabre, T. Duong, H. Buc, U. Nehrbass, J.C. Olivo-Marin, O. Gadal, and C. Zimmer. 2008. High-resolution statistical mapping reveals gene territories in live yeast. *Nat. Methods*. 5:1031–1037. http://dx.doi.org/10.1038/nmeth.1266

Therizols, P., T. Duong, B. Dujon, C. Zimmer, and E. Fabre. 2010. Chromosome arm length and nuclear constraints determine the dynamic relationship of yeast subtelomeres. *Proc. Natl. Acad. Sci. USA*. 107:2025–2030. http://dx.doi.org/10.1073/pnas.0914187107

Codes (MATLAB scripts) of custom-made software tracking loci are available as a ZIP file.